Int. J. Nano Dimens., 8 (2): 142-158, Spring 2017

ORIGINAL ARTICLE

Theoretical calculations of solvation 12-Crown-4 (12CN4) in aqueous solution and its experimental interaction with nano $CuSO_4$

Laila I. Ali; Shimaa Abdel Halim; Sameh Gamal Sanad*

Department of Chemistry, Faculty of Education, Ain Shams University, Roxy 11711, Cairo, Egypt

Received 25 January 2017; revised 29 March 2017; accepted 05 April 2017; available online 11 April 2017

Abstract

Theoretical study of the electronic structure, and nonlinear optical properties (NLO) analysis of 12-crown-4 were done using Density Functional Theory (DFT) evaluations at the B3LYP/6-311G (d, p) level of theory. The optimized structure is nonlinear compound as indicated from the dihedral angles were presented. The calculated E_{HOMO} and E_{LUMO} energies of 12-Crown-4 (12CN4) can be used to explain the charge transfer in 12-Crown-4 (12CN4) and to calculated the global properties; the chemical hardness (η), softness (S) and electronegativity (χ). The NLO parameters: static dipole moment (μ), polarizability (α), anisotropy polarizability ($\Delta\alpha$) and first order hyperpolarizability (β_{tot}) of the 12-Crown-4 (12CN4) have been calculated at the same level of theory. The molecular electrostatic potential (MEP) and electrostatic potential (ESP) for the title molecule were investigated and analyzed. Also the electronic absorption spectra were measured in ethanol and water solvents and the assignment of the observed bands has been discussed by time-dependent density functional theory (TD-DFT) calculations. The correspondences between calculated and experimental transitions energies are satisfactory. From the experimental conductance measurements, the association thermodynamic parameters (K_A, ΔG_A, ΔH_A and ΔS_A) and complex formation thermodynamic parameters (K_f, ΔG_f, ΔH_f and ΔS_f) for nano-$CuSO_4$ in presence of 12-crown-4 (12CN4) as chelating agent in 10% ethanol – water solvents at different temperatures (298.15, 303.15, 308.15 and 313.15K) were applied and calculated.

Keywords: *Association parameters; DFT/TD-DFT; Formation parameters; Nano-$CuSO_4$; NLO analysis; UV-spectra; 12-Crown-4.*

How to cite this article

Ali I L, Abdel Halim Sh, Sanad G S., Theoretical calculations of solvation 12- Crown-4 (12CN4) in aqueous solution and its experimental interaction with nano $CuSO_4$. Int. J. Nano Dimens., 2017; 8(2): 142-158., DOI: 10.22034/ijnd.2017.24995

INTRODUCTION

Crown ethers were discovered by Pederson in 1967 [1], and became the first synthetic ligands to demonstrate selectivity for metal ions. Crown ethers have a hydrophilic cavity (HC) delineated by a lipophilic portion of the molecule. Crown ethers have been studied extensively [2], and it was determined that their structures were comparable to certain antibiotics like Valinomycin [3] or Enunciation [4]. These structural similarities led to the use of crown ethers as reference models to study the binding and delivery mechanism of these antibiotics to their target sites [5]. Gas phase conformational analyses of 12CN4 [6–8] were reported previously. However, consideration of solvent solute interactions [9] is essential, and the distributional treatment of thermodynamic properties in each phase will substantially improve the results and the accuracy of conclusion . Since the seminal work on self-consistent reaction fields (SCRF) by Onsager [10], there has been a tremendous amount of research done on the theoretical framework for solution phase studies [11]. This implicit solvation model approach is popular because it allows the calculation of the properties of a molecule in solution without prohibitively expensive computational cost. Even with the reduced computational cost, the geometry optimization of relatively large molecule such as crown ether requires significant amount of computational resource. The empirical geometrical parameters of solute in aqueous

* Corresponding Author Email: Shimaaquantum@ymail.com

solution could not only provide the benchmark to the theory but also assist the reduction of computational resource [12].

The NLO properties depend on the extent of charge transfer (CT) interaction across the conjugative paths and the electron transfer ability of an aromatic ring and on its ionization potential (IP) and electron affinity (EA) [13, 14]. Linear Polarizability ($\Delta\alpha$) and first order Hyperpolarizability (β) are required for the rational design of optimized materials for photonic devices such as electro optic modulators and all-optical switches [15, 16]. In these study our contribution here is to shed more light on the geometric structure (bond lengths, bond angles and dihedral angles), ground state properties of 12-crown-4 (12CN4) using Density Functional Theory (DFT-B3LYP) and basis set 6-311G (d,p), and nonlinear optical (NLO) analysis are performed to identify and characterize the forces that govern the structure of the title molecule. In addition to investigate the effect of solvent polarity on the observed spectra and hence, predicting the relative stabilities, extent of charge transfer character and assignment of the observed electronic transitions bands as localized, delocalized and/or of charge transfer (CT) has been facilitated by Density Functional Theory (DFT) and time-dependent density functional theory (TD-DFT) calculations. The electronic structure of molecules usually manifests itself in the electronic absorption and emission spectra. This manifestation enables the detailed understanding of the forces that govern the electronic structure of the studied compound 12-crown-4(12CN4).

Copper sulfate is a fungicide material. Some of fungi able to elevates levels of copper ions. Algae can be controlled with small copper sulfate concentration. Copper sulfate inhibits growth of bacteria. Copper sulfate can cause cell death which through apoptosis and necrosis [17, 18].

EXPERIMENTAL

Preparation of materials

In 5 ml of the nano-$CuSO_4$ solution (1.0×10^{-3} M) and solution of 12-crown-4 (12CN4) (1.0×10^{-4} M) were placed in the titration cell, thermo stated at the preset temperature and the conductance of the solution was measured after the solution reached thermal equilibrium. Then, a known amount of solvent was added in a stepwise manner using a calibrated micropipette. The conductance of the solution was measured after each addition until the desired constant reading was achieved. The specific conductance values were recorded using conductivity bridge JENCO–3173 COND, with a cell constant equal to 1, temperatures were adjusted at 298.15, 303.15, 308.15 and 313.15K [19, 20].

Computational method

Calculations have been performed using Khon-Sham's Density Functional Theory (DFT) method subjected to the gradient-corrected hybrid density functional B3LYP method [21]. This function is a combination of the Becke's three parameters non-local exchange potential with the non-local correlation functional of Lee et al [22]. For each structure, a full geometry optimization was performed using this function [22] and the 6-311G (p,d) basis set [23] as implemented by Gaussian 09 package [24]. All geometries were visualized either using Gauss View 5.0.9 [25] or chemcraft 1.6 software packages. No symmetry constrains were applied during the geometry optimization. Also, the total static dipole moment (μ), ($\Delta\alpha$), (β) values were calculated by using the following equations [26- 28]:

$$\mu = (\mu^2_x + \mu^2_y + \mu^2_z)^{1/2},$$
$$(\alpha) = 1/3\,(\alpha_{xx} + \alpha_{yy} + \alpha_{zz}),$$
$$\Delta\alpha = ((\alpha_{xx} - \alpha_{yy})^2 + (\alpha_{yy} - \alpha_{zz})^2 + (\alpha_{zz} - \alpha_{xx})^2/2)^{1/2},$$
$$(\beta) = (\beta^2_x + \beta^2_y + \beta^2_z)^{1/2}, \quad (1)$$

Where

$$\beta_x = \beta_{xxx} + \beta_{xyy} + \beta_{xzz},$$
$$\beta_y = \beta_{yyy} + \beta_{xxy} + \beta_{yzz},$$
$$\beta_z = \beta_{zzz} + \beta_{xxz} + \beta_{yyz}. \quad (2)$$

By using HOMO and LUMO energy values for a molecule, electronegativity, and chemical hardness can be calculated as follows: $\chi = (I + A)/2$ (electronegativity), $\eta = (I - A)/2$ (chemical hardness), $S = 1/2\eta$ (chemical softness) where I and A are ionization potential and electron affinity, and $I = -E_{HOMO}$ and $A = -E_{LUMO}$, respectively [29, 30]. The conversion factors for α, β, γ, and HOMO and LUMO energies in atomic and cgs units: 1 atomic unit (a.u.) = 0.1482×10^{-24} electrostatic unit (esu) for polarizability; 1 a.u. = 8.6393×10^{-33} esu for first hyperpolarizability; 1 a.u. = 27.2116 eV (electron volt) for HOMO and LUMO energies.
Solvents: Ethanol obtained from Ai-Nasr Co., 98%, and was used without further purification. Second distilled water was also used. Apparatus: Conductivity bridge JENCO – 3173 COND.

RESULTS AND DISCUSSION

Association thermodynamic parameters

The association constants for nano-$CuSO_4$ in the presence of ligand 12-crown-4 in ethanol and water at different temperatures (298.15, 303.15, 308.15 and 313.15K) were calculated by using equation (4) [31-36].

$$K_A = \Lambda_0 \frac{\Lambda_0 - S(Z)\Lambda_m}{C_m \Lambda_m{}^2 S(Z)^{2\gamma\pm 2}} \quad (3)$$

Where (Λ_m, Λ_0) are the molar and limiting molar conductance of nano- $CuSO_4$ in presence of ligand respectively, C_m is the molar concentration of nano- $CuSO_4$, S(Z) is Fouss – Shedlovsky factor, equal unity for strong electrolytes, $\gamma_\pm$ is the mean activity coefficient.

The association constants, free energies, association constants and degree of dissociation in presence of 12-crown-4 for nano- $CuSO_4$ at different temperatures are tabulated in Tables (1 and 2) descript (Association constants at different temperatures, free energies, enthalpies and entropies of association for nano $CuSO_4$ interacted with 12-crown-4 (12CN4) at 10% EtOH-H_2O solvents). The relation between Λ_m(molar conductance) and $C^{1/2}$ in presence of 12-crown-4 for nano- $CuSO_4$ at different temperatures is shown in Fig. 1. The relation between log K_A and 1/T in presence of 12-crown-4 (12CN4) for nano-$CuSO_4$ is shown in Fig. 2.

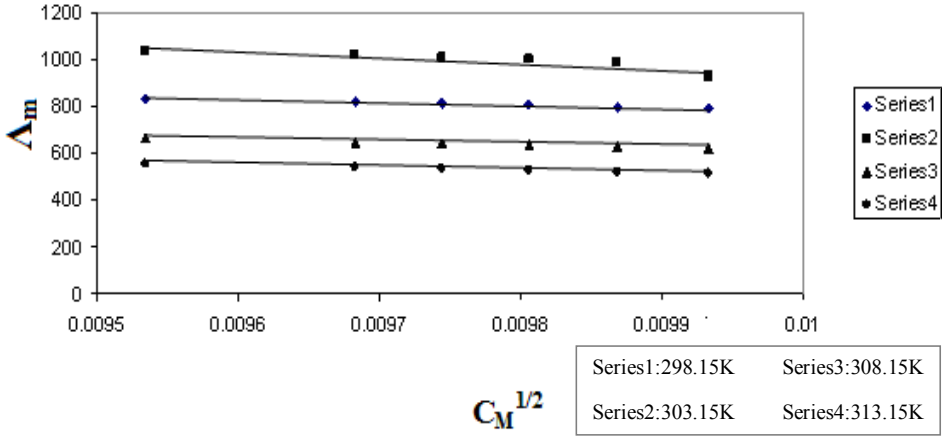

Fig. 1: The relation between Λ_m and $C^{1/2}$ in presence of 12-crown-4 (12CN4) plus nano- $CuSO_4$ at different temperatures.

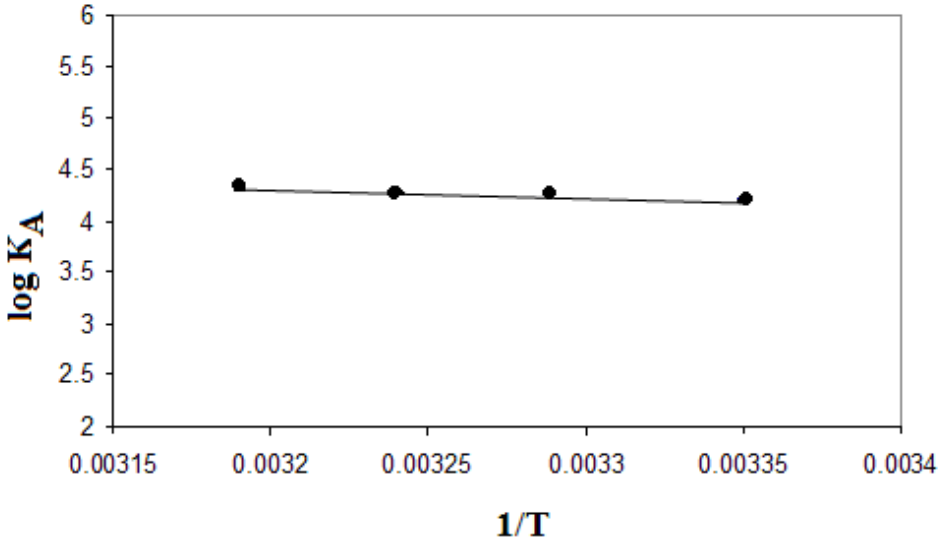

Fig. 2: The relation between log K_A and 1/T in presence of 12-crown-4 (12CN4) plus nano- $CuSO_4$.

Table 1: Association constants at different temperatures for nano $CuSO_4$ interacted with 12-crown-4 (12CN4) at 10% EtOH-H_2O solvents.

T (K)	C	$C^{1/2}$	Λ_m	Λ_0	Log $\gamma_\pm$	$\gamma_\pm$	K_A
298.15	9.091×10^{-5}	0.0095	833.692	1500	-0.0048	0.977	16573.03
303.15	9.091×10^{-5}	0.0095	1035.73	2250	-0.0048	0.977	29352.94
308.15	9.091×10^{-5}	0.0095	666.593	1250	-0.0048	0.977	18915.03
313.15	9.091×10^{-5}	0.0095	553.294	1100	-0.0048	0.977	22640.27

Table 2: Association constants, free energies, enthalpies and entropies of association for nano $CuSO_4$ interacted with 12-crown-4 (12CN4) at 10% EtOH-H_2O solvents.

T (K)	ΔG_A	ΔH_A	$T\Delta S$	ΔS_A
298.15	-24.0882	73.1038	97.192	0.326
303.15	-25.9331	73.1038	99.0369	0.3267
308.15	-25.2348	73.1038	98.3386	0.3191
313.15	-26.1124	73.1038	99.2162	0.3168

Formation thermodynamic parameters

The relations between molar conductance (Λ_m) and the molar ratio of metal to ligand (M/L) elucidate the formation of 1:2 and 1:1 stoichiometric complexes. The formation constants (K_f) for the complexes were calculated for each type of complexes 1:2 and 1:1 (M:L) by using equation (5) [37- 40].

$$K_f = \frac{\Lambda_M - \Lambda_{obs}}{\Lambda_{obs} - \Lambda_{ML}\,[L]} \quad (4)$$

Where Λ_M is the limiting molar conductance of the salt alone, Λ_{obs} is the molar conductance of solution during titration and Λ_{ML} is the molar conductance of the complex. The free energies of formation and formation constants for nano-$CuSO_4$ in 10% ethanol - 90% water mixed solvents at different temperatures in presence of 12-crown-4 (12CN4) are tabulated in Table (3). Descript (Formation constants, free energies, enthalpies and entropies of formation for nano $CuSO_4$ interacted with 12-crown-4 (12CN4) at 10% EtOH-H_2O solvents). The relations between Λ_m and [M]/[L] in case of using 12-crown-4 chelating agent are constructed at 10% ethanol - 90% water at different temperatures and the results are shown in Figs. 3-6. Relations between log K_f and 1/T for nano-$CuSO_4$ in presence of 12-crown-4 by different ratios of metal to ligand (M:L) in ethanol-water mixed solvents are shown in Figs. 7 and 8.

TEM for nano-$CuSO_4$ is show in Fig. 9 (a-d). In all pictures (a-d) measured by using JEOL HRTEM – JEM 2100 (JAPAN) show that TEM of $CuSO_4$ obtained in ethanol are irregular spheres in the form of cylinders. The diameter is in the range of 10-77.86 nm. The small sizes in the range between 10, 12.05 to 20.76 nm are collected to give bigger sizes till 77.86 nm (a-c). These different sizes were proved also by x- ray diffraction which gave crystal sizes in the same order (d) .The non homogeneity in sizes for nano copper sulfate need controlling during the primary preparation of the samples.

Ground state properties

The total energy (E_T), energy of highest occupied molecular orbital (E_{HOMO}), energy of lowest unoccupied molecular orbital (E_{LUMO}), energy gap (E_g) and dipole moment (μ) of of the studied ligand compound 12-crown-4 (12CN4) are presented in Table (4). The optimized structure of the title molecule is obtained using the B3LYB/6-311G (p,d) level, numbering system, net charge, vector of dipole moment and the charge density maps of HOMO and LUMO are presented in Fig. 10 descript (Optimized geometry, numbering system, vector dipole moment (a), net charge (b) HOMO

and LUMO (c) for ligand 12-Crown-4 (12CN4) using B3LYP/6-311G (d, p)). From Table (4) and Fig. 10 one can reveal the following:

The ionization energy, I.E, of compound 12-crown-4 (12CN4) which measures the donating property (oxidation power) is 6.64 eV (c.f. Table 4). Also the electron affinity (E.A) which measures the accepting property (reducing power) is 1.20 eV. So the calculated energy gaps, (Eg), which measure the chemical activity, of compound free 12-crown-4 is 5.44 eV (≈ 125.5 kcal). Finally, the theoretically computed dipole moment (μ), which measures the polarity or charge separation over the title molecule, is 2.46 D.

Geometric Structure

The optimized geometric parameters (bond lengths, bond angles and dihedral angles) of the title molecules using B3LYP/6-311G (d, p) level of theory are listed in Table (5), and are compared with the available x-ray experimental data [41]. The observed bond lengths of C_1-C_8, C_1-O_{11} and C_1-H_{24} in 12-crown-4(12CN4) are 1.513 Å, 1.414 Å and 1.096 Å respectively, while the obtained theoretical values are 1.503 Å, 1.414 Å and 1.082 Å respectively [41]. The computed bond angles of $<C_3O_{10}C_4$, $<O_{11}C_2H_{25}$, $<C_1H_{23}H_{24}$, and $<C_2C_3H_{27}$ are 116.49°, 106.05°, 107.26° and 111.19° respectively, while the experimental values are 116.71°, 106.45°, 107.56° and 112.19° respectively. In conclusion, the bond lengths and angles calculated by B3LYP methods are in good agreement with the experimental values. The Mullikan net charge observed on active centers O_1, O_2, O_3, and O_4 are -0.360, -0.371, -0.372 and -0.388 respectively. The most stable geometry of the studied compound is non-planar structure as indicated from the dihedral angles (c.f. Table 5).

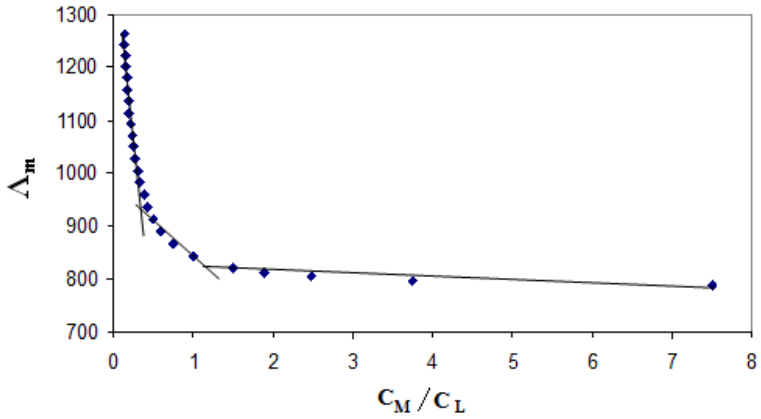

Fig. 3: The relation between Λ_m and C_M/C_L at 298.15K of 12-crown-4 (12CN4) plus nano- $CuSO_4$.

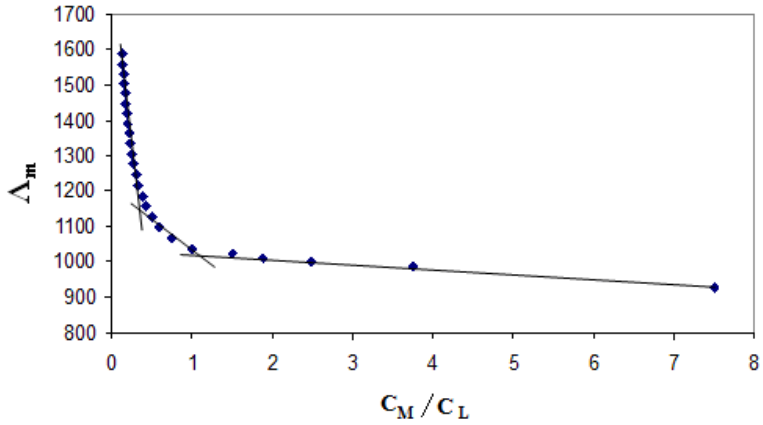

Fig. 4: The relation between Λ_m and C_M/C_L at 303.15K of 12-crown-4 (12CN4) plus nano- $CuSO_4$.

Table 3: Formation constants, free energies, enthalpies and entropies of formation for nano $CuSO_4$ interacted with 12-crown-4 (12CN4) at 10% EtOH-H_2O solvents.

TEMP	M:L	K_f	ΔG_f	ΔH_f	ΔS_f
298.15	1:2	5379.561	-22.1873	-7.0844	0.0507
	1:1	55912.750	-22.063	-7.0844	0.0494
303.15	1:2	6324.774	-22.3172	-7.0844	0.0494
	1:1	68546.760	-21.6574	-7.0844	0.0465
308.15	1:2	6059.717	-27.4103	-19.3003	0.0272
	1:1	66544.800	-28.0703	-19.3003	0.0289
313.15	1:2	4684.044	-28.4573	-19.3003	0.0297
	1:1	61040.34	-28.2361	-19.3003	0.0285

Table 4: Total energy, energy of HOMO and LUMO, energy gap and dipole moment of ligand 12-crown-4 (12CN4) computed at the B3LYP/6-311G (d,P) level of theory.

Compounds	E_T (au)	E_{HOMO} (eV)	E_{LUMO} (eV)	E_{gap} (eV)	μ (Debye)
12-Crown-4	-615.48455	-6.63898	-1.196528	5.442452	2.4626

Table 5: Selected experimental and theoretical bond lengths, bond angles and dihedral angles for ligand 12-crown-4 (12CN4) at the B3LYP/6-311G (d,P) level of theory.

Bond lengths (Å)	12-Crown-4	X-ray [41]	Bond angle (°)	12-Crown-4	X-ray [41]	Dihedral angles (°)	12-Crown-4	X-ray [41]
C_1 –C_8	1.503	1.513	$<C_6O_9C_5$	114.918	115.011	$O_{11}C_1C_8O_{12}$	-68.881	-63.841
C_1 – O_{11}	1.414	1.414	$<C_2O_{11}C_3$	112.835	112.835	$O_{11}C_1C_8H_{21}$	48.382	49.382
C_1 – H_{23}	1.090	1.104	$<C_3O_{10}C_4$	116.493	116.713	$O_{11}C_1C_8H_{22}$	167.867	170.017
C_1 – H_{24}	1.082	1.096	$<C_1O_{11}C_8$	109.022	109.622	$H_{23}C_1C_8O_{12}$	53.024	55.024
C_2 – C_3	1.513	1.513	$<O_{11}C_1H_{23}$	110.866	112.008	$H_{23}C_1C_8H_{21}$	170.287	170.387
C_2 – O_{11}	1.430	1.431	$<C_1H_{23}H_{24}$	107.256	107.556	$H_{23}C_1C_8O_{12}$	-70.228	-73.728
C_2 – H_{25}	1.082	1.098	$<C_2H_{25}H_{26}$	108.111	108.031	$C_8C_1O_{11}C_2$	153.644	155.674
C_2 – H_{26}	1.090	1.107	$<C_5H_{15}H_{16}$	109.135	109.135	$H_{23}C_1O_{11}C_2$	31.875	33.075
C_3 – O_{10}	1.423	1.419	$<O_{11}C_2H_{25}$	106.052	106.452	$H_{24}C_1O_{11}C_2$	-86.839	-85.839
C_3 – H_{27}	1.082	1.099	$<C_2C_3H_{27}$	111.191	112.191	$H_{27}C_3O_{10}C_4$	25.964	-0.796
C_3 – H_{28}	1.090	1.106	$<C_3O_{10}C_4$	119.620	119.620	$H_{28}C_3O_{10}C_4$	-93.316	-95.316
C_4 – O_{10}	1.420	1.418	$<C_1O_{11}C_2$	117.995	117.995	$C_7C_6O_9C_5$	100.948	146.948
C_4 – H_{13}	1.090	1.100	$<C_7O_{12}C_8$	118.801	118.801	Net charges		
C_5 – O_9	1.440	1.440				O_1	-0.360	
C_5 – H_{16}	1.082	1.099				O_2	-0.371	
C_6 – C_7	1.501	1.509				O_3	-0.372	
C_6 – H_{17}	1.090	1.104				O_4	-0.388	
C_6 –H_{18}	1.090	1.102						
C_8 – O_{12}	1.423	1.428						
C_4 – O_{10}	1.421	1.428						

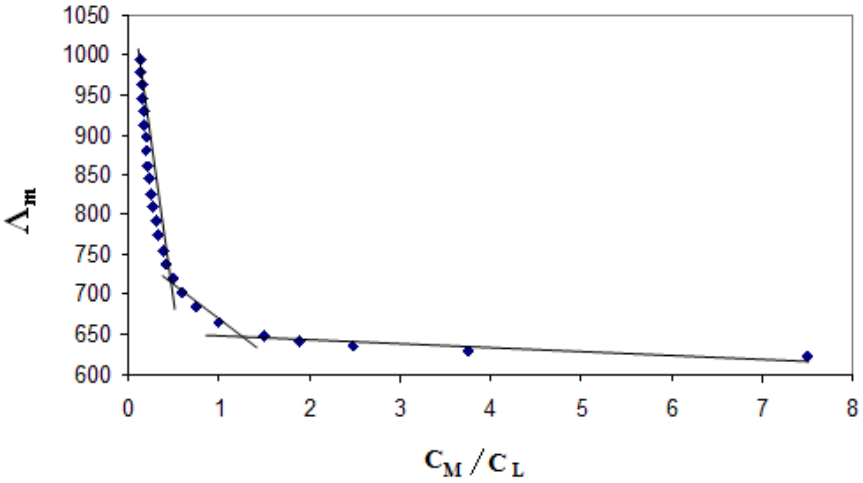

Fig. 5: The relation between Λ_m and C_M/C_L at 308.15K of 12-crown-4 (12CN4) plus nano- $CuSO_4$.

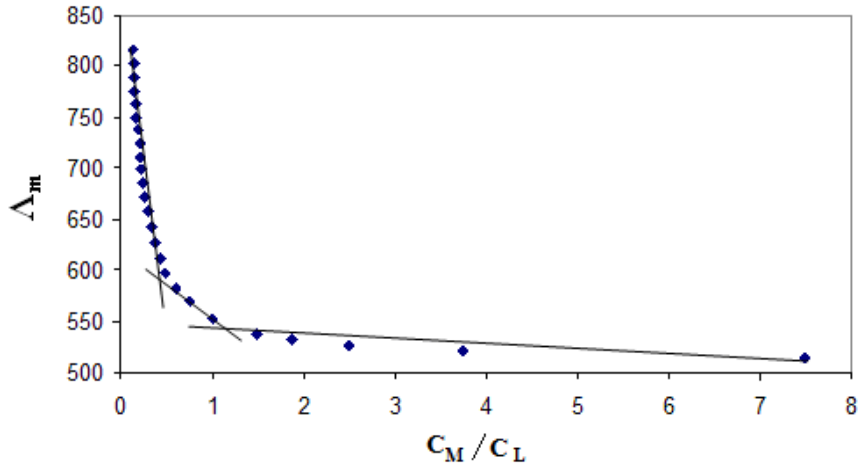

Fig.6: The relation between Λ_m and C_M/C_L at 313.15K of 12-crown-4 (12CN4) plus nano- $CuSO_4$.

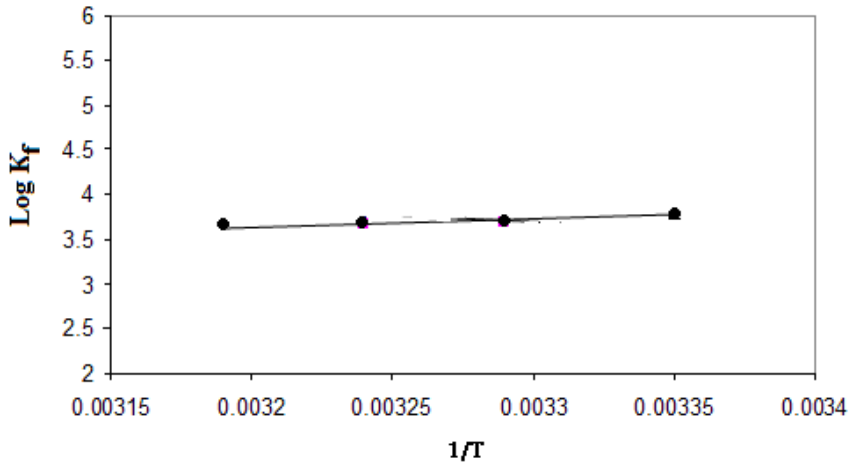

Fig. 7: Relation between $\log K_f$ and 1/T when M:L is 1:2 of 12-crown-4 (12CN4) plus nano- $CuSO_4$.

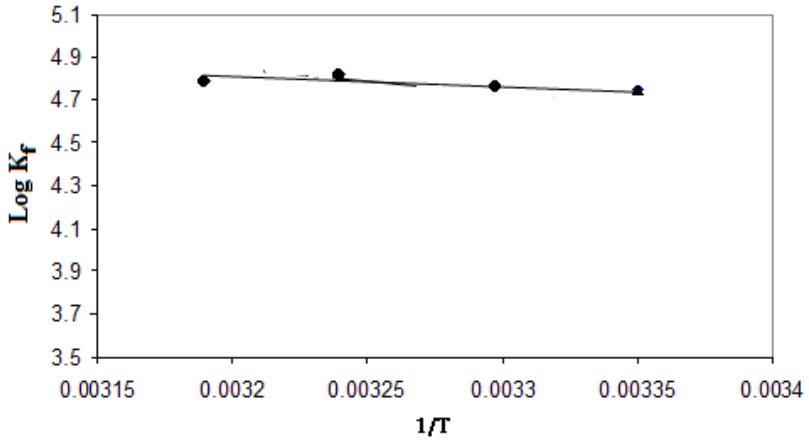

Fig. 8: Relation between logKf and 1/T when M:L is 1:1 of 12-crown-4 (12CN4) plus nano- $CuSO_4$.

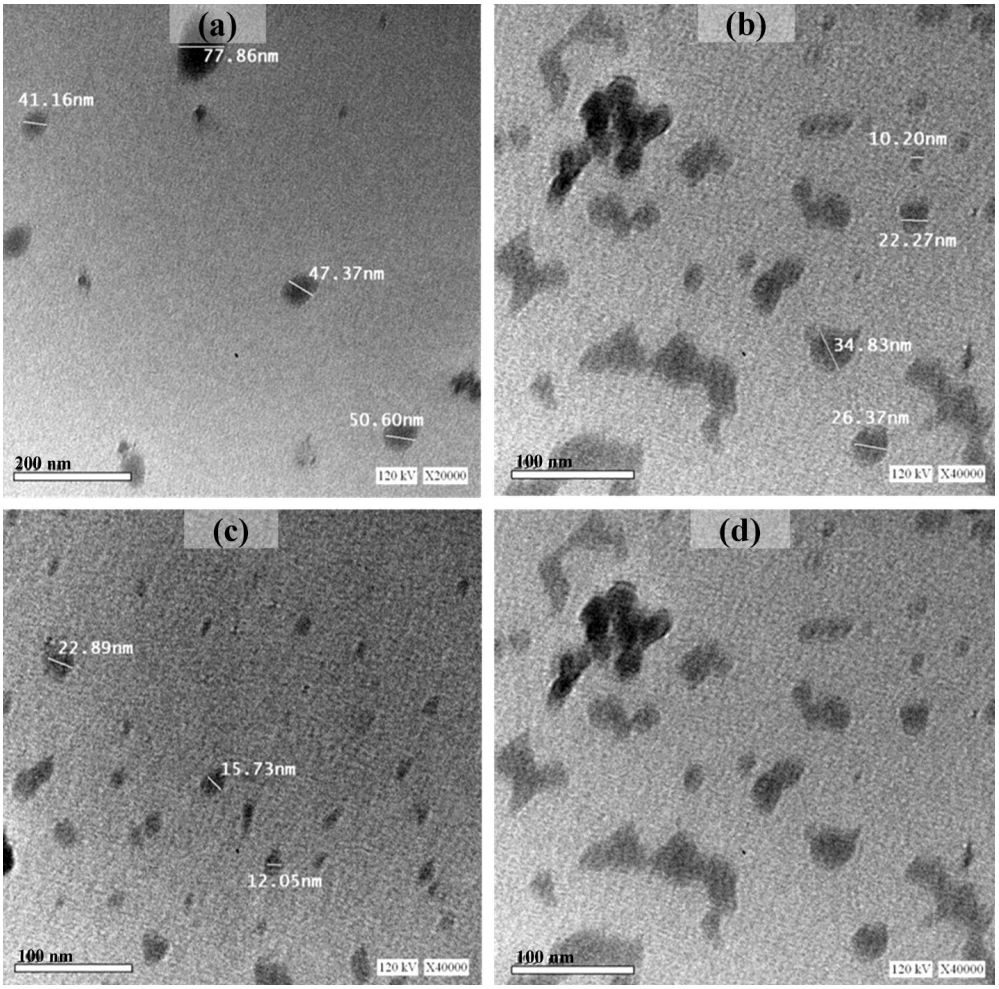

Fig. 9: In all images (a-d) measured by using JEOL HRTEM – JEM 2100 (JAPAN) show that TEM of $CuSO_4$ obtained in ethanol are irregular spheres in the form of cylinders. The diameter in the range of 10-77.86 nm. The small sizes in the range between 10, 12.05 to 20.76 nm are collected to give bigger sizes till 77.86 nm (a-c). These different sizes were proved also by x- ray diffraction which gave crystal sizes in the same order (d). The non homogeneity in sizes for Nano copper sulfate needs controlling during the primary preparation of the samples.

Global reactivity descriptors

The frontier molecular orbital (FMO) energies of the title molecule were calculated using B3LYP/6-311G (d, p). HOMO energy characterizes the electron giving ability, while LUMO energy characterizes the electron withdrawing ability. Energy gap between HOMO and LUMO characterizes the molecular chemical stability and it is a critical parameter in determining molecular electrical transport properties because it is a measure of electron conductivity. From Fig. 10 (Optimized geometry, numbering system, vector dipole moment (a), net charge (b) HOMO and LUMO (c) for ligand 12-Crown-4 (12CN4) using B3LYP/6-311G (d, p)), and Table (6), (The ionization potential (I /eV), electron affinity (A / eV), chemical hardness (/ eV), softness (S/ eV^{-1}), chemical potential (μ) and electronegativity (/eV), of ligand 12-Crown-4 (12CN4) using B3LYP/6-311G (d, P)). HOMO energy is calculated as -6.63898 eV and LUMO energy is calculated as −1.196528 eV by using B3LYP/6-311G (d, p) level. The small energy gap between HOMO and LUMO indicated that charge transfer occurs within the title molecule and the molecule can be easily polarized. Using HOMO and LUMO energies ionization potential and electron affinity can be explicated as $IP \approx -E_{HOMO,}$ $EA \approx -E_{LUMO.}$ The variation of electro negativity (χ) values is supported by the electrostatic potential. For any two molecules, electron will be partially transferred from one of low χ to that of high χ (electron flow from high chemical potential to low chemical potential). The chemical hardness (η) = ($IP - EA$)/2, electro negativity (χ) = ($IP + EA$)/2, chemical potential (μ) = - ($IP + EA$)/2, and chemical softness (S) = 1/2η, values were calculated as 2.721, 3.917, -3.917 and 0.184 respectively.

Obtained small η value means that the charge transfer occurs in the molecule. Considering the η values, large HOMO – LUMO gap means a hard molecule and small HOMO – LUMO gap means a soft molecule. Additionally, it can be said that the small HOMO – LUMO energy gap represents more reactive molecule.

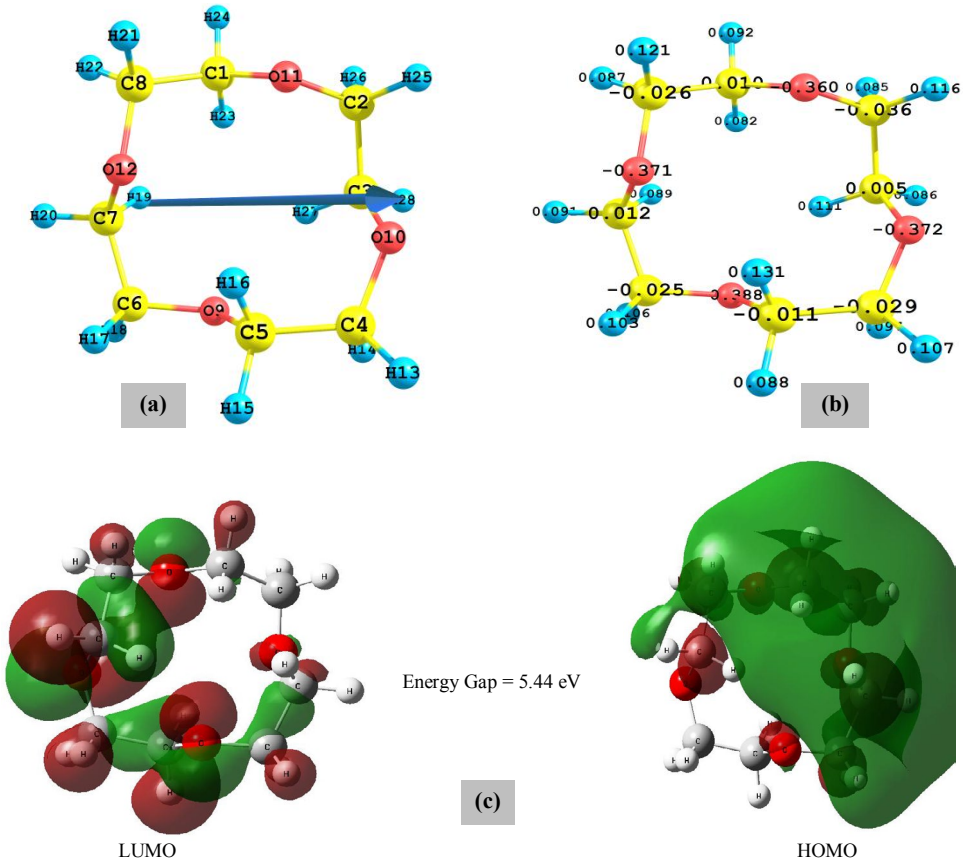

Fig. 10: Optimized geometry, numbering system, vector dipole moment (a), net charge (b) HOMO and LUMO (c) for ligand 12-crown-4 (12CN4) using B3LYP/6-311G (d, p).

Other molecular properties

The 3D plots of highest occupied molecular orbital (HOMO) and the lowest unoccupied molecular orbital (LUMO), electrostatic potential (ESP), electron density (ED), and the molecular electrostatic potential map (MEP) for the title molecule at the B3LYP method with 6-311G (d, p) level are shown in Figs. (10 and 11). The ED plot for the title molecule shows a uniform distribution. While the negative ESP is localized more over the oxygen atoms, the positive ESP is localized on the rest of the title molecule. MEP has been used primarily for predicting sites and relative reactivity's towards electrophilic and nucleophilic attack, and in studies of biological recognition and hydrogen bonding interactions [42-44]. The calculated 3D MEP of the title compound was calculated from optimized molecular structure by using B3LYP/6–311G (d, p) level and also shown in Fig. 11 Descript (Molecular surfaces (a - c) and atomic charge distribution (au) (d) of the ligand 12-Crown-4(12CN4) using B3LYP/6-311G (d, p)).

Table 6: The ionisation potential (I /eV), electron affinity (A /eV), chemical hardness (χ/eV), softness (S/ eV-1), chemical potential (μ) and electronegativity (η/eV), of ligand 12-crown-4 (12CN4) using B3LYP/6-311G (d, P).

Compounds	*I (eV)*	*A(eV)*	*X(eV)*	*(eV) μ*	*η(eV)*	*S(eV^{-1})*
12-Crown-4	6.639	1.196	3.917	3.917-	2.721	0.184

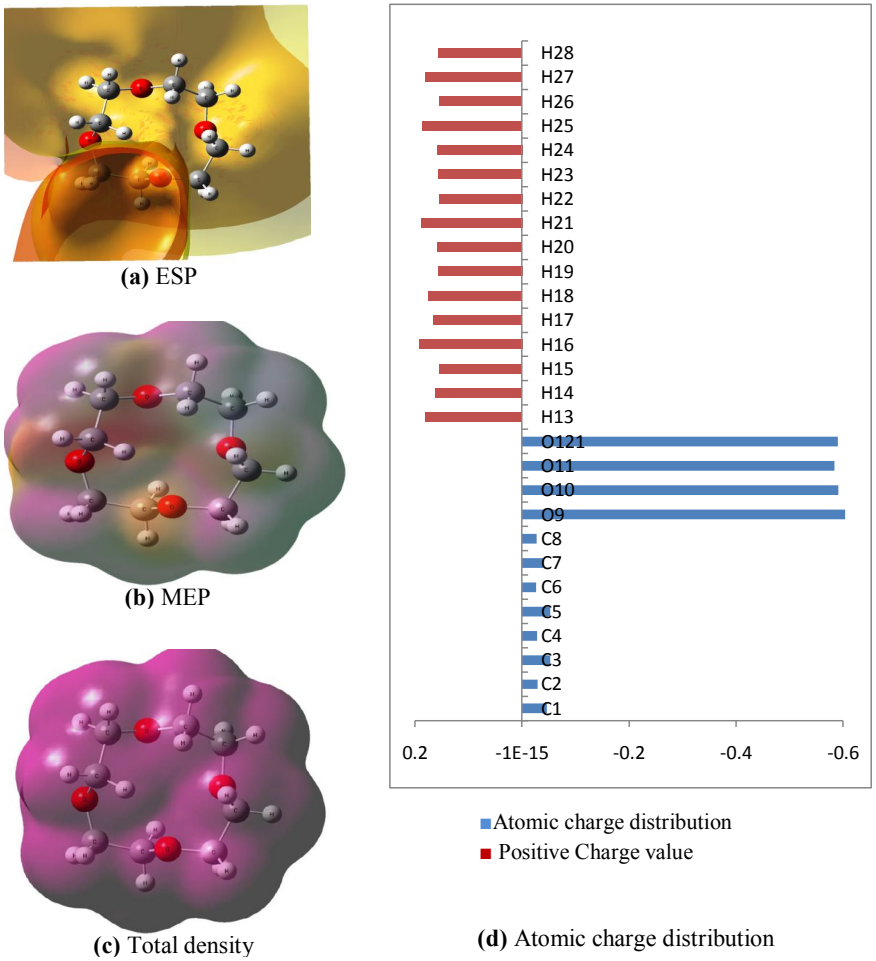

(a) ESP

(b) MEP

(c) Total density

(d) Atomic charge distribution

Fig. 11: Molecular surfaces (a - c) and atomic charge distribution (au) (d) of the ligand 12-crown-4 (12CN4) using B3LYP/6-311G (d, p).

The color scheme for the MEP surface is as follows: red for electron rich, partially negative charge; blue for electron deficient, partially positive charge; light blue for slightly electron deficient region; yellow for slightly electron rich region; green for neutral (zero potential); respectively. According to our results, the negative region (red) is mainly over the O atomic sites, which were caused by the contribution of lone-pair electrons of oxygen atom while the positive (blue) potential sites are around the hydrogen and carbon atoms. A portion of a molecule that has a negative electrostatic potential will be susceptible to electrophilic attack—the more negative is the better. It is not as straightforward to use electrostatic potentials to predict nucleophilic attack [45]. Hence, the negative region (red) and positive region (blue) indicate electrophilic and nucleophilic attack symptoms. Also, a negative electrostatic potential region is observed around the O_9 atom. The corresponding Mulliken's plot with B3LYP/6-311G (d, p) method are shown in Fig. 11. It is noted that from Fig. 11, the strong negative and positive partial charges on the skeletal atoms (especially O_9, O_{10}, C_1, C_2, O_{11}, O_{12}, C_3, C_4, C_5, C_6, C_7, C_8, H_{17}, H_{18}, H_{24}, H_{25}) for the selected compounds increase with increasing Hammett constant of substituent groups [46, 47]. These distributions of partial charges on the skeletal atoms show that the electrostatic repulsion or attraction between atoms can give a significant contribution to the intra- and intermolecular interaction.

Nonlinear optical (NLO) Analysis

P-nitroaniline (PNA) is one of the prototypical molecules used in the study of the NLO properties of molecular systems. In this study, the typical NLO material, PNA was chosen as a reference molecule; because there were no experimental values about the title compound in the literature. The relatively NLO of the title molecule compared to PNA indicate their promising applications in NLO materials. Therefore it was used frequently as a threshold value for comparative purposes and still continues to be a recognized prototype of organic NLO chromophores. Its hyperpolarizability was studied both experimentally and theoretically in various solvents and at different frequencies [48–51]. Polarizabilities and hyperpolarizabilities characterize the response of a system in an applied electric field [52]. They determine not only the strength of molecular interactions as well as the cross-sections of different scattering and collision processes, but also the non-linear optical (NLO) properties of the system [53-56] In order to investigate the relationships among photocurrent generation, molecular structures and NLO, the polarizabilities and hyperpolarizabilities of title compound was calculated using B3LYP method, 6-311G (d, p) basis set, based on the finite-field approach. The mean first order hyperpolarizability (β), total static dipole moment (μ), the mean polarizability (<α>), and the anisotropy of the polarizability (Δα), of title molecule are presented in Table (7) descript (Total static dipole moment (μ), the mean Polarizability (<α>), the anisotropy of the Polarizability (Δα), and the mean first-order Hyperpolarizability (<β>) for ligand 12-Crown-4(12CN4) using B3LYP/6-311G (d, P)). The calculated value of dipole moment was found to be 2.4549 D at B3LYP/6-311G (d, p). The calculated mean polarizability (<α>) is $6.97x10^{-24}$esu i.e. two times smaller than PNA molecule. In addition, the calculated mean first order Hyperpolarizability (β), of the title molecule is $1.36x10^{-30}$ esu i.e. smaller than PNA molecule [57-59]. This result indicates the linearity of the title molecule and promising the title molecule to be not used as NLO materials.

Electronic absorption spectra of the title compound 12-crown-4.

The electronic spectra of compound 12-crown-4 in ethanol and water solvents and the assignment of spectra are given in Figs. (12 and 13) descript (Electronic absorption spectra of ligand compound 12-Crown-4(12CN4), theoretical and experimental) and Table (8) descripts (Theoretical and experimental UV spectra of ligand 12-Crown-4(12CN4), calculated at TD-B3LYP/6–311G (d, p)).

The charge density maps of the occupied and vacant MO's considered in the transitions is presented in Fig. 14 descript (charge density maps of the occupied (a - d) and unoccupied (e - v) of ligand compound 12-Crown-4(12CN4). The spectrum in ethanol and water is composed of four bands centered at 170, 173 nm, 160, 162 nm, 147, 149 nm, and 139, 141 nm. Increasing solvent polarity causes small changes in band positions indicating that the polarity of the excited and ground state are of the same values, that is, solvent independent. All bands are assigned to (π-π*) transitions as reflected from their intensities (0-35000).

Table 7: Total static dipole moment (μ), the mean polarizability (<α>), the anisotropy of the Polarizability (Δα), and the mean first-order Hyperpolarizability (<β>) for ligand 12-crown-4 (12CN4) using B3LYP/6-311G (d, P).

Property	PNA	B3LYP/6-311G(d,P) 12-Crown-4
μ_x		1.6035 Debye
μ_y		-0.1257 Debye
μ_z		1.8545 Debye
μ	2.44 Debye [a]	2.4549 Debye
α_{XX}		-70.6119 a.u.
α_{XY}		0.8373 a.u.
α_{YY}		-68.7589 a.u.
α_{ZZ}		-74.9054 a.u.
α_{YZ}		4.4892 a.u.
α_{XZ}		0.2072 a.u.
<α>	22×10^{-24} cm[3b]	6.97×10^{-24} esu
Δα		2.11×10^{-24} esu
βxxx		10.3187 a.u.
βxxy		-0.7192 a.u.
βxyy		1.8876 a.u.
βyyy		-2.0991 a.u.
βxxz		7.9585 a.u.
βxyz		-6.5738 a.u.
βyyz		-4.0989 a.u.
βxzz		-1.6175 a.u.
βyzz		-0.4451 a.u.
βzzz		-4.4668 a.u.
<β>	15.5×10^{-30} esu[c]	1.36×10^{-30} esu

[a, b, c] PNA results are taken from references [57-59].

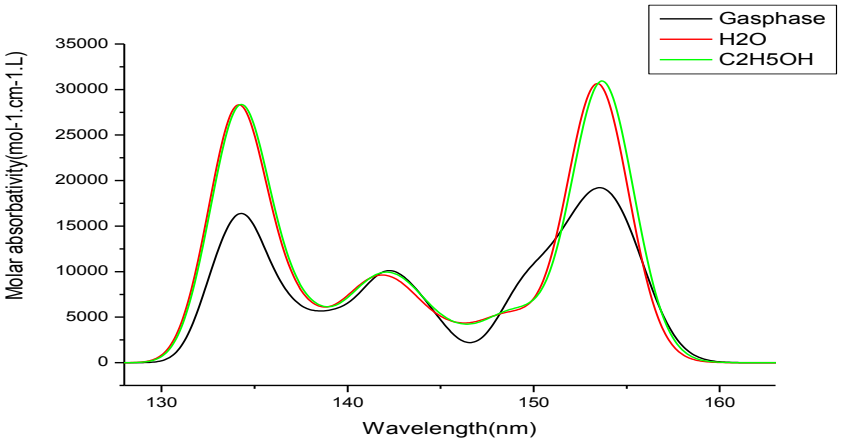

Fig. 12: Electronic absorption spectra of ligand 12-crown-4 (12CN4), theoretical.

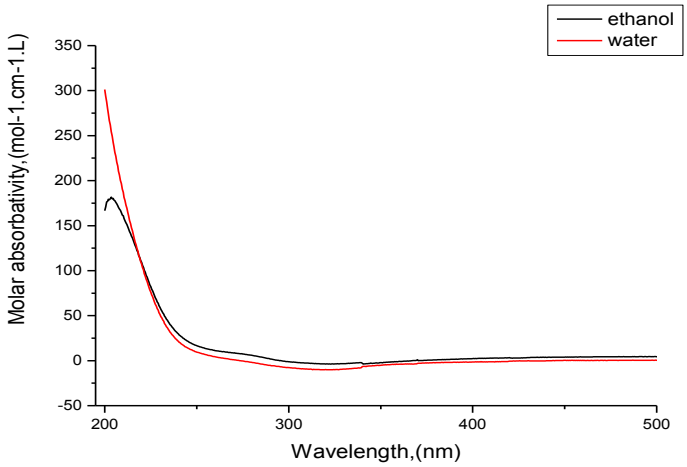

Fig. 13: Electronic absorption spectra of ligand 12-crown-4 (12CN4), experimental.

Table 8: Theoretical and experimental UV spectra of ligand 12-crown-4 (12CN4), calculated at TD-B3LYP/6–311G (d, p).

	TD-Theoretical												Experimental	
	Gas phase				Water				Ethanol				Ethanol	Water
state	Configuration	Coefficient	f	λ, nm	Config uration	Coefficient	f	λ, nm	Configuration	Coefficient	f	λ, nm	λ, nm	λ, nm
I	46-> 49	0.41	0.04	159	45-> 49	0.12	0.11	153	45-> 49	-0.1	0.11	154	170	173
	47->49	0.26			46->49	-0.2			46->49	0.15				
	47->50	-0.2			46->51	0.17			46->51	0.2-				
	47->51	0.13			46->53	-0.1			47-> 49	0.49				
	48-> 49	0.3-			47-> 49	0.48			47-> 50	-0.1				
	48->50	0.11			47->50	0.1-			48->50	-0.1				
	48->51	-0.2			48->50	0.12			48->51	0.26				
					48->51	-0.3								
II	45-> 49	-0.2	0.06	157	45-> 51	-0.1	0.11	153	45-> 51	-0.1	0.11	153	160	162
	46->49	-0.3			46->49	-0.3			46->49	-0.3				
	46->50	-0.2			46->50	0.12			46->50	0.12				
	46->51	0.10			47->49	0.1-			47-> 49	0.13				
	47-> 49	0.46			47-> 53	0.11			47-> 53	-0.1				
	47->50	0.12			48->50	0.44			48->50	0.45				
	48->50	0.17			48->51	0.21			48->51	0.22				
II I	45-> 50	0.11	0.07	155	45-> 49	0.15	0.11	134	45-> 49	0.1-	0.11	134	147	149
	46->49	0.22			45->53	-0.1			45->53	0.11				
	46->52	0.10			46->50	-0.1			46->50	0.12				
	47->50	0.16			46->51	-0.1			46->51	0.11				
	48-> 49	0.15			46-> 53	0.13			46-> 53	0.1-				
	48->50	0.19			46->61	-0.1			46->61	0.11				
	48->51	0.46			47->50	0.10			47->50	0.10				
	48->52	0.17			47->53	0.25			47->53	0.24				
	48->53	0.2-			47->54	0.15			47->54	0.15				
					47-> 55	0.10			47-> 55	0.10				
					48->55	0.11			48->55	-0.1				
					48->60	-0.2			48->60	0.18				
					48-> 62	0.12			48-> 62	-0.1				
					48->63	0.18			48->63	-0.2				
					48->64	0.11			48->64	-0.1				
					48->65	-0.1			48->65	0.11				
I V	45-> 50	0.18	0.03	144	45-> 49	0.15	0.04	135	45-> 49	0.17	0.04	135	139	141
	45->51	0.13			45->51	0.17			45->51	0.16				
	46->50	0.31			45->52	0.10			46->52	0.13				
	46->52	0.2-			46->52	0.14			46->54	0.1-				
	47-> 49	0.18			46-> 54	0.1-			47->56	0.14				
	47->50	-0.1			47->56	0.1-			47->58	0.2-				
	47->51	0.11			47->58	0.18			47->59	0.11				
	47->52	0.10			47->59	0.1-			48->50	0.11				
	47->53	0.3-			48->50	0.11			48->52	0.30				
	47->54	0.13			48->52	0.30			48->54	-0.2				
	48->52	0.11			48->54	-0.2			48->58	-0.2				
	48->53	0.10			48->58	-0.2								

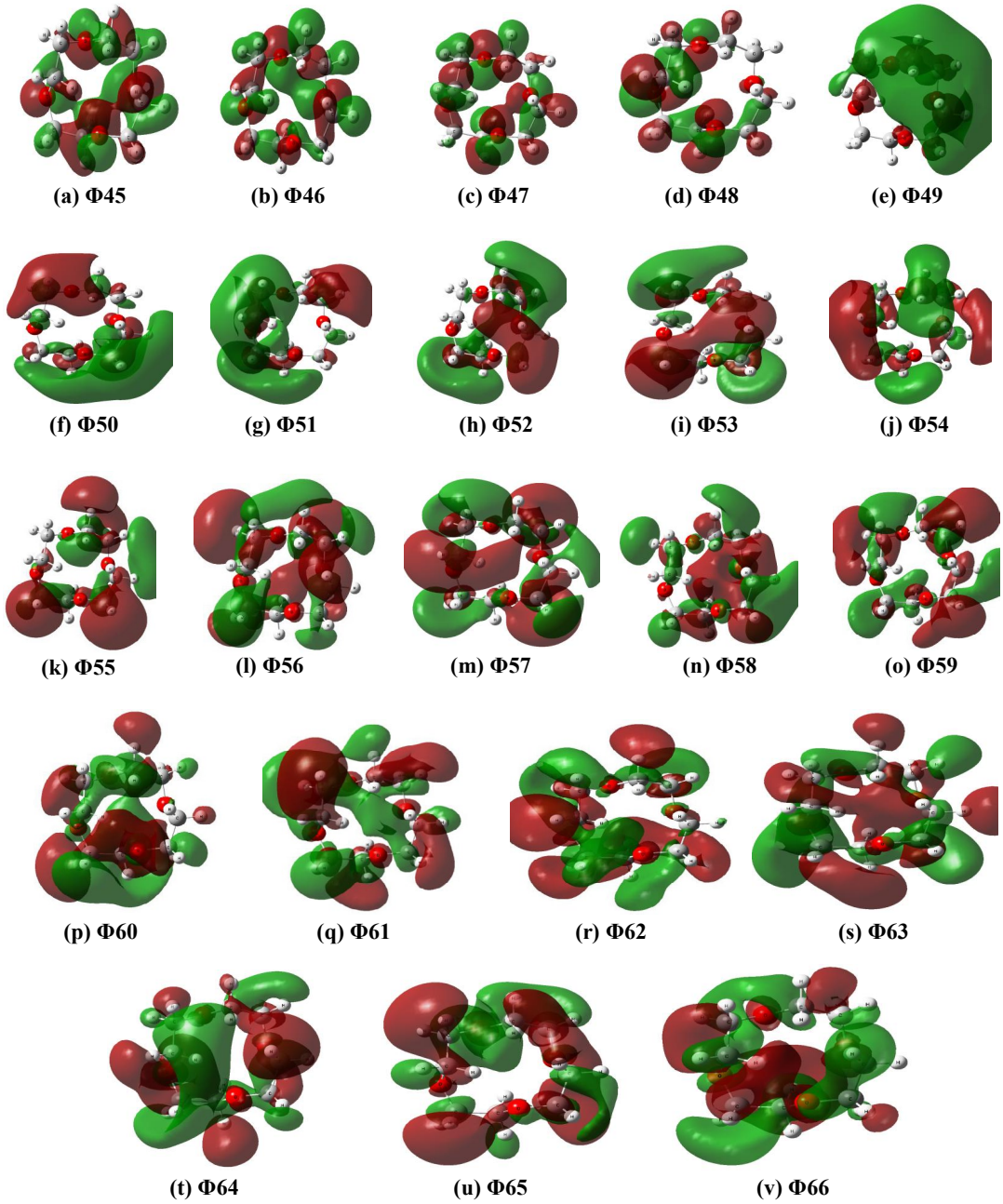

Fig. 14: The charge density maps of the occupied (a - d) and unoccupied (e - v) of ligand 12-crown-4 (12CN4).

The excited configurations considered in compound 12-crown-4(12CN4) are those which results from an electron excitation of four highest occupied molecular orbital's $\phi_{45}^{-1}\phi_{48}$ and the lowest 18 vacant molecular orbital's $\phi_{49}^{-1}\phi_{66}$. The correspondence between the theoretically computed and the experimentally observed transitions are satisfactory. The first $(\pi\text{-}\pi^*)^1$ state is centered at 170, 173 nm in ethanol and water this band is predicted theoretically at 159, 154, 153 nm, in very good agreement with the experiment and is composed of a mixture of seven configurations, (c.f. Table 8) and assigned as CT, localized and delocalized configurations may be expected. The second $(\pi\text{-}\pi^*)^1$ state is observed at 160, 162 nm in ethanol and water and is predicted theoretically at 157, 153, 153 nm. This state is composed of a mixture of seven configurations, namely, $\phi_{45}^{-1}\phi_{49,}$

$\phi_{46}^{-1}\phi_{49}$, $\phi_{46}^{-1}\phi_{50}$, $\phi_{46}^{-1}\phi_{51}$, $\phi_{47}^{-1}\phi_{49,}$ $\phi_{47}^{-1}\phi_{50}$ and $\phi_{48}^{-1}\phi_{50}$, that is, delocalized configurations and CT character may be expected (Fig. 14).

The third $(\pi\text{-}\pi^*)^1$ state is observed in ethanol and water at 147, 149 nm and predicted theoretically at 155, 134, 134 nm. This band is composed of a mixture of nine configurations, (Table 8) and assigned as CT character and delocalized band. The main contribution of this band is coming from the one configuration ϕ^{-1}_{48} ϕ_{51}, which is of CT character may be expected (Fig. 14). The finally $(\pi, \pi^*)^1$ state computed at 139, 141 nm in ethanol and water, and is computed theoretically at 144, 135, 135 nm. This state possesses a high polarity as compared to that of the ground state and hence solvent dependence on band position is expected. This state is composed of a mixture of 12 configurations, which is also assigned as a delocalized, localized, and a charge transfer band (CT) (Fig. 14).

CONCLUSION

The molecular geometry of compound 12-crown-4 (12CN4) in the ground state has been calculated by using density function theory (DFT-B3LYP/6-311G (d,p) level of theory. The optimized structure of the molecule is nonplanar as indicated from the dihedral angles. The HOMO-LUMO energy gap helped in analyzing the chemical reactivity, hardness, softness, chemical potential and electronegativity. Mullikan and natural charge distribution of the molecule 12-crown-4(12CN4) were studied which indicated the electronic charge distribution in the molecule 12-crown-4(12CN4). The calculated dipole moment and first order hyperpolarizability results indicate that the molecule 12-crown-4(12CN4) has a reasonable good linear optical behavior. MEP confirmed the different negative and positive potential sites of the molecule in accordance with the total electron density surface. All the observed bands in the UV spectra can be assigned to $(\pi\text{-}\pi^*)$ transitions as reflected from their intensities. The correspondence between the theoretically computed and the experimentally observed transitions are satisfactory. The solvent dependence of the observed bands can be attributed to the change in the transition dipole moments of the ground and excited states. According to the high activity in physical parameters of 12-crown-4 E_{HOMO}, E_{LUMO}, E_{gap} and dipole moment (μ) was applied for the interaction with nano $CuSO_4$ solutions in 10% ethanol –water solvents form 1:1 and 1:2 M/L complexes with increasing of the thermodynamic parameters, Gibbs free energies, enthalpies and entropies of solvation by increasing of temperature indicating more interactions. The association and complex formation parameters between nano $CuSO_4$ and 12-crown-4 (12CN4) were discussed.

CONFLICT OF INTEREST

The authors declare that there is no conflict of interests regarding the publication of this manuscript.

REFERENCES

[1] Pedersen C. J., (1967), Crystalline salt complexes of macrocyclic polyethers. *J. Am. Chem. Soc.* 89: 385-391.

[2] Arnaud-Neu F., Delgado R., Chaves S., (2003), Critical evaluation of stability constants and thermodynamic functions of metal complexes of crown ethers. *Pure. Appl. Chem.* 75: 71-102.

[3] Wong P. S. H., Antonio B. J., Dearden D. V., (1994), Gas-Phase studies of valinomycin-alkali metal cation complexes: Attachment rates and cation affinities. *J. Am. Soc. Mass Spectrosc.* 5: 632 - 637.

[4] Andreas T., Tsatsas R. W., Stearns W., Risen M., (1972), Nature of alkali metal ion interactions with cyclic polyfunctional molecules. I. Vibrations of alkali ions encaged by crown ethers in solution. *J. Am. Chem. Soc.* 94: 5247- 5253.

[5] Popov A. I., Lehn J. M., Melson G. A., (Ed.), (1979); Coordination Chemistry of Macrocyclic Compounds, Plenum, New York, 537: Lamb J. D., Izatt R. M., Christensen J. J., Eatough D.J., Melson G. A., (Ed.), (1979) Coordination Chemistry of Macrocyclic Compounds, Plenum, New York, 145.

[6] Hay B. P., Rustad J. R., Zipperer J. P., Wester D. W., (1995), Topological electron density analysis of organosulfur compounds. *J. Mol. Struct.* 337: 201-207.

[7] El-Azhary A. A., Al-Kahtani A. A., (2004), Conformational study of the structure of free 12-Crown-4. *J. Phys. Chem. A*. 108: 9601-9607.

[8] El-Azhary A. A., Al-Kahtani A. A., (2005), Experimental and theoretical study of the vibrational spectra of free 12-Crown-4. *J. Phys. Chem. A*. 109: 4505-4511.

[9] Hori K. N., Dou K., Okano A., Ohgami Tsukube H., (2002), Stable of 12-crown-O$_3$N and its Li$^+$ complex in aqueous solution. *J. Comp. Chem.* 23: 1226-1235.

[10] Onsager L., (1936), Electric Moments of Molecules in Liquids. *J. Am. Chem. Soc.* 58: 1486-1493.

[11] Cramer C. J., Truhlar D. G., (1999), Implicit solvation models: Equilibria, structure, spectra, and dynamics. *Chem. Rev.* 99: 2261-2200.

[12] Tanika A., Hashim A., William A. B., Eiko K., Hideya K., (2011), Theoretical and ATR-FTIR study of free 12-crown-4 in aqueous solution. *Chem. Phys. Letts.* 502: 253-258.

[13] Mandal K., Kar T., Nandi P. K., Bhattacharyya S. P., (2003), Theoretical study of the nonlinear polarizabilities in H_2N and NO_2 substituted chromophores containing two hetero aromatic rings. *Chem. Phys. Letts.* 376: 116-124.

[14] Nandi P. K., Mandal K., Kar T., (2003), Effect of structural changes in sesquifulvalene on the intramolecular charge transfer and nonlinear polarizations: A theoretical study. *Chem. Phys. Letts.* 381: 230-238.

[15] Prasad P. N., Williams D. J., (1991), Introduction to Nonlinear Optical Effects in Molecules and Polymers. *John Wiley & Sons*, New York, NY, USA.

[16] Meyers F., Marder S. R., Pierce B. M., Brédas J. L., (1994), Electric field modulated nonlinear optical properties of donor-acceptor polyenes: Sum-over-states investigation of the relationship between molecular polarizabilities (*Alpha., Beta. and Gamma.*) and bond Length Alternation. *J. Am. Chem. Soc.* 116: 10703-10714.

[17] Holleman A. F., Wiberg E., (2001), Inor. Chem., San Diego: Acad. Press. ISBN 0-12-352651-5.

[18] David A., (2002), Wright and Pamela Welbourn Environmental Toxicology, Cambridge University Press, UK.

[19] El Sayed M., Abou E., Esam A. G., (2013), Thermodynamics of Solvation for Nano Zinc Oxide in 2 MNH4Cl+ Mixed DMF – H_2O Solvents at Different Temperatures. Int. J. Eng. Innov. Tech. 2: 121-126.

[20] Esam A., Gomaa A., (2014), Thermodynamics of complex formation (Conductometrically) between Cu (II) ion and 4-Phenyl -1- Diacetyl Monoxime –3 Thiosemicarbazone (BMPTS) in methanol at different temperatures. *J. Sys. Sci.* 3: 12-25.

[21] (a) Becke A., (1993), Densityfunctional thermochemistry. III. The role of exact exchange. *Chem. Phys.* 98: 5648-5652.

[22] Lee C., Yang W., Parr R. G., (1988), Development of the Colle-Salvetti correlation-energy formula into a functional of the electron density. *Phys. Rev. B. Condens. Matter.*157: 785-789.

[23] Stefanov B, Liu B. G., Liashenko A., Piskorz P., Komaromi I., Martin R. L., Fox D. J., Keith T., Al-Laham M. A., Peng C. Y., Nanayakkara A., Challacombe M., Gill P. M. W., Johnson B., Chen W., Wong M. W., Gonzalez C., Pople J. A., (2003), Gaussian, Inc., Pittsburgh P. A.

[24] Frisch M., Trucks J. G. W., Schlegel H. B., Scuseria G. E., (2009), Gaussian, Inc., Wallingford CT.

[25] Dennington K. R., Millam T., Semichem J., (2009), Gauss View, Version 5 Inc., Shawnee Mission KS.

[26] Avci D., (2011), Second and third-order nonlinear optical properties and molecular parameters of azo chromophores: Semiempirical analysis. *Spectrochimica Acta A.* 82: 37-43.

[27] Avci D., Başoğlu A., Atalay Y., (2010), NLO and NBO analysis of sarcosine maleic acid by using HF and B3LYP calculations. *Struct. Chem.* 21: 213-219.

[28] Avci D., Cömert H., Atalay Y., (2008), Ab initio Hartree-Fock calculations on linear and second-order nonlinear optical properties of new acridine-benzothiazolylamine chromophores. *J. Mol. Modeling.* 14: 161-171.

[29] Pearson R. G., (1986), Absolute electronegativity and hardness correlated with molecular orbital theory. *Proc. Nat. Acad. Sci.* 83: 8440-8441.

[30] Chandra A. K., Uchimara T., (2001), NLO and NBO analysis of sarcosine-maleic acid by using HF and B3LYP calculations. *J. Phy. Chem. A*. 105: 3578-3582.

[31] Szafran M., Komasa A., Bartoszak-Adamska E., (2007), Crystal and molecular structure of 4-carboxypiperidinium chloride (4-piperidinecarboxylic acid hydrochloride). *J. Mol. Struct.* 827: 101-107.

[32] Ives D. J. G., (1971), Chemical thermodynamics, university chemistry, maconald technical and scientific.

[33] Dickenson R. E., Geis I., Benjamin Chemistry W. A., (1976), Matter, and the Universe, Inc., USA.

[34] Oswal S. L., Desai J. S., Ijardar S. P., Jain D. M., (2009), Studies of partial molar volumes of alkylamine in non-electrolyte solvents II. Alkyl amines in chloroalkanes at 303.15 and 313.15 K. *J. Mol. Liquids*. 144: 108 - 114.

[35] Zhang D. E., Zhang X. J., Ni X. M., Zheng H. G., Yang D. D., (2005), Synthesis and characterization of $NiFe_2O_4$ magnetic nanorods via a PEG-assisted route. *J. Magn. Mater*. 292: 79-82.

[36] Xia B. Y., Yang P. D., Sun Y. G., (2003), One-dimensional nanostructures: Synthesis, characterization, and applications. *Adv. Mater*. 15: 353-356.

[37] Duan X., Huang Y., Cui Y., Wang J., Lieber C. M., (2001), Indium phosphide nanowires as building blocks for nanoscale electronic and optoelectronic devices. *Nature.* 409: 66-69.

[38] Mohamed N. H., Hamed Esam A., Gomaa S. G., Sanad A., (2014), Thermodynamics of solvation for nano zinc carbonate in mixed DMF-H_2O solvents at different temperatures. *Int. J. Eng. Innov. Tech. (IJEIT).* 4: 203-207.

[39] Liu W. J., He W. D., Zhang Z. C., (2006), Nanogenerators-from scientific discovery to future applications. *J. Cryst. Growth*. 290: 592-598.

[40] Yizahak M., (1990), Solubility and solvation in mixed solvent systems. *Pure and Applied Chem.* 62: 2069-2076.

[41] Chen L., Shen L., Xie A., Zhu J., Wu Z., Yang L., (2007), Discovery of diamond in eclogite from the Chinese Continental Scientific Drilling Project Main Hole (CCSD-MH) in the Sulu UHPM belt [in Chinese]. *Cryst. Res. Technol.* 42: 886-891.

[42] Yurii A., Simonov A., Alexandr D., Marina S., Fonari T., Malinowski I., Elzbieta L., Andrzej C., Jan F., Biernat V. E., Ganin P., (1993), Investigation of structural, thermal and magnetic behaviors of pristine barium carbonate nanoparticles synthesized by chemical Co-Precipitation method. *J. Inclusion Phen. Molec. Recognition in Chem.* 15: 79-85.

[43] Snehalatha M., Ravikumar C., Hubert Joe I., Sekar N., Jayakumar V. S., (2009), Vibrational spectra and scaled quantum chemical studies of the structure of Martius yellow sodium saltmonohydrate. *Spectrochim. Acta. A.* 72: 1121-1126.

[44] Scrocco E., Tomasi J., (1979), Interpretation by means of electrostatic molecular potentials. Adv. Quant. Chem. 11: 115-120.

[45] Luque F. J., López J. M., Orozco M., (2000), Electrostatic interactions of a solute with a continuum. A direct utilization of ab initio molecular potentials for the prevision of solvent effects. *Theoret. Chem. Accounts,* 103: 343-345.

[46] Okulik N., Jubert A. H., (2005), Theoretical analysis of the reactive sites of non-steroidal anti-inflammatory drugs. *Int. Elect. J. Mol. Des.* 4: 17-30.

[47] Politzer P., Murray J. S., (2002), The fundamental nature and role of the electrostatic potential in atoms and molecules. *Theor. Chem. Acc.* 108: 134-142.

[48] Sajan D., Joseph L., Vijayan N., Karabacak M., (2011), Natural bond orbital analysis, electronic structure, non-linear properties and vibrational spectral analysis of l-histidinium bromide monohydrate: A density functional theory. *Spectrochim. Acta A*. 81: 85-98.

[49] Hansch C., Leo A., Taft R. W., (1991), A survey of Hammett substituent constants and resonance and field parameters. *Chem. Rev.* 91: 165-195.

[50] Jensen L., Van Duijnen P. T., (2005), The first hyperpolarizability of p-nitroaniline in 1, 4-dioxane: A quantum mechanical/molecular mechanics study. *J. Chem. Phys.* 123 Article ID 074307.

[51] Sałek P., Vahtras O., Helgaker T., Ågren H., (2002),

Density-functional theory of linear and nonlinear time-dependent properties molecular. *J. Chem. Phys.* 117: 9630-9635.

[52] Stähelin M., Burland D. M., Rice J. E., (1992), Sign change of hyperpolarizabilities of solvated water. *Chem. Phys. Lett.* 191: 245-250.

[53] Huyskens F. L., Huyskens P. L., Persoons A. P., (1998), Solvent dependence of the first hyperpolarizability of p-nitroanilines: Differences between nonspecific dipole–dipole interactions and solute-solvent H-bonds. *J. Chem. Phys.* 108: 8161-8168.

[54] Zhang C. R., Chen H. S., Wang G. H., (2004), Geometry, electronic structure, and related properties of dye sensitizer: 3,4-bis[1-(carboxymethyl)-3-indolyl]-1H-pyrrole-2, 5-dione. *Chem. Res. Chin. U*. 20: 640-646.

[55] Sun Y., Chen X., Sun L., Guo X., Lu W., (2003), A monolayer organic light-emitting diode using an organic dye salt. *Chem. Phys. Lett.* 83: 1020-1022.

[56] Christiansen O., Gauss J., Stanton J. F., (1999), Non-Linear Optical Properties of Matter. *Chem. Phys. Lett.* 305: 51-99.

[57] Cheng L. T., Tam W., Stevenson S. H., Meredith G. R., Rikken G., Marder S. R., (1991), Experimental investigations of organic molecular nonlinear optical polarizabilities. 1. Methods and results on benzene and stilbene derivatives. *J. Phys. Chem.* 95: 10631-10643.

[58] Karna S. P., Prasad P. N., Dupuis M., (1991), Nonlinear optical properties of novel thiophene derivatives: Experimental and ab initio time-dependent coupled perturbed Hartree–Fock studies. *J. Chem. Phys.* 94: 1171-1179.

[59] Kaatz P., Donley E. A., Shelton D. P., (1998), A comparison of molecular hyperpolarizabilities from gas and liquid phase measurements. *J. Chem. Phys.* 108: 849-855.